BEILSTEIN JOURNAL OF NANOTECHNOLOGY

Pinning of a ferroelectric Bloch wall at a paraelectric layer

Vilgelmina Stepkova* and Jiří Hlinka

Full Research Paper

Open Access

Address:
Institute of Physics, The Czech Academy of Sciences, 182 21 Prague, Czech Republic

Email:
Vilgelmina Stepkova* - stepkova@fzu.cz

* Corresponding author

Keywords:
$BaTiO_3$–$SrTiO_3$ superlattices; ferroelectric domain walls; Ginzburg–Landau–Devonshire model; phase-field simulations

Beilstein J. Nanotechnol. **2018,** *9,* 2356–2360.
doi:10.3762/bjnano.9.220

Received: 07 April 2018
Accepted: 09 August 2018
Published: 31 August 2018

Associate Editor: U. D. Schwarz

Abstract

The phase-field simulations of ferroelectric Bloch domain walls in $BaTiO_3$–$SrTiO_3$ crystalline superlattices performed in this study suggest that a paraelectric layer with a thickness comparable to the thickness of the domain wall itself can act as an efficient pinning layer. At the same time, such a layer facilitates the possibility to switch domain wall helicity by an external electric field or even to completely change the characteristic structure of a ferroelectric Bloch wall passing through it. Thus, ferroelectric Bloch domain walls are shown to be ideal nanoscale objects with switchable properties. The reported results hint towards the possibility to exploit ferroelectric domain wall interaction with simple nanoscale devices.

Introduction

Nanometer-scale mixtures of paraelectric and ferroelectric materials in disordered solid solutions or in very fine artificial crystalline superlattices often show qualitatively similar domain phenomena as the parent ferroelectric materials. For example, in the case of $BaTiO_3$–$SrTiO_3$ superlattices with only a few atomic layers of $SrTiO_3$, the domain walls are simply expected to penetrate through $BaTiO_3$/$SrTiO_3$ interfaces [1-5]. In general, it can be expected that a small amount of paraelectric defects, smaller or thinner than the correlation length, will not substantially alter the superposed domain structure in a strong ferroelectric material like $BaTiO_3$. In other words, a sufficiently thin paraelectric layer is effectively polarized by the neighboring ferroelectric material. However, little is known about robustness of the inner polarization, present within the nanoscale thickness of ferroelectric Bloch walls [6,7]. For example, it has not yet been clarified whether such a localized polarization is sustained under the influence of the chemical stoichiometry concentration fluctuations typical for relaxor ferroelectric perovskites, for example. Similarly, we are not aware of any device geometries that can define or alter the helicity of Bloch walls.

In order to assess the interaction of Bloch walls with material inhomogeneities, we have explored the limiting case of ferroelectric Bloch walls encountering a layer of paraelectric material by means of phase-field simulation. This technique allows the relaxed domain wall profiles to be predicted by simulated annealing of the system based on numerical solution of material-specific time-dependent Ginzburg–Landau–Devonshire equations [8-10]. It is intuitively clear that a paraelectric layer would act as pinning loci for the Ising ferroelectric wall because the

interior of an Ising wall is not polarized at all. In that respect, the largest effect is expected for a layer with thickness matching that of the domain wall. Therefore, we have considered a hypothetical $BaTiO_3$–$SrTiO_3$ crystalline superlattice, formed by thin $SrTiO_3$ paraelectric layers of 0.5–3 nm thickness, separated by about 13 nm thick $BaTiO_3$ ferroelectric slabs (see Figure 1). The $SrTiO_3$ layers were normal to the $[\bar{2}11]$ crystallographic direction, common to the parent cubic lattice of both $BaTiO_3$ and $SrTiO_3$.

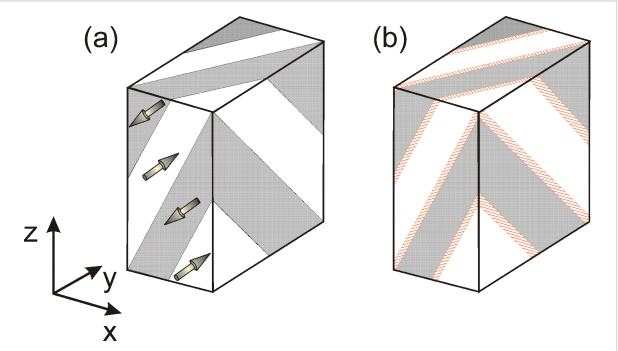

Figure 1: Domain structure with $[\bar{2}11]$-oriented 180-degree domain walls in a) pure $BaTiO_3$, b) $BaTiO_3$–$SrTiO_3$ superlattice with $SrTiO_3$ layers situated within the domain walls. Shaded areas correspond to $[111]$ polarized domains, unshaded areas represent $[\bar{1}\bar{1}\bar{1}]$ domains. Hatched regions in b) correspond to $SrTiO_3$ layers.

It is found that a nanometer thin layer of $SrTiO_3$ acts as a pinning loci not only for the Ising wall but also for the Bloch wall. Moreover, these results suggest that such a pinned Bloch wall can loose practically all of its inner polarization (see Figure 2). This result could be possibly used to set or modify the helicity of Bloch walls passing through conveniently placed paraelectric gate layers in future domain-wall-based devices.

Results and Discussion

The peculiarity of the investigated ferroelectric domain wall is best understood when the polarization is expressed in the symmetry-adapted Cartesian system [6] associated with the set of orthogonal unit vectors **r** || [111], **s** || $[\bar{2}11]$, and **t** || $[0\bar{1}1]$. By definition [6], the adjacent domains differ in the sign of the P_r component. In the case of Ising walls, the integral of the P_t component across a given wall is zero. In the case of Bloch walls, there is an overall polarization in the P_t component within the few nanometer thickness of the given domain wall itself. This inner polarization can be negative or positive.

The relaxed, equilibrium polarization profile in the simulation for pure $BaTiO_3$ is shown in Figure 3. The nonzero P_t peak located at the wall implies that these domain boundaries are indeed Bloch walls. The alternating sign of the P_t component in subsequent domain walls indicates that the energetically equivalent Bloch walls present in this simulation have the same helicity. For comparison, Figure 4 shows the profile of the Ising domain wall, which is obtained by the same simulation but under an epitaxial compressive stress of 3.0 GPa, applied in the plane perpendicular to the spontaneous polarization as described in [11].

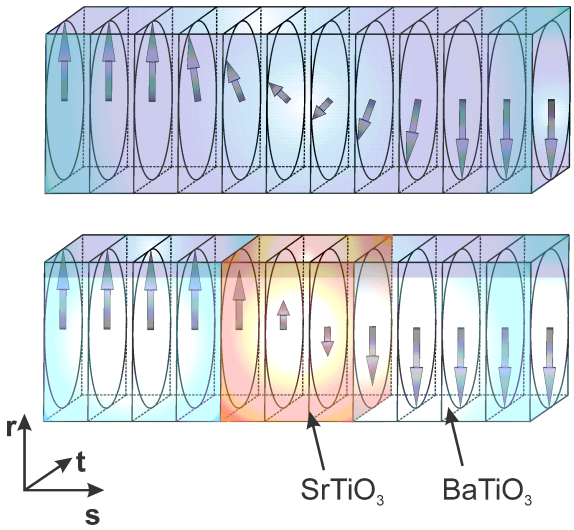

Figure 2: Schematic illustration of polarization passing across the 180-degree domain wall in pure rhombohedral $BaTiO_3$ and in the superlattice containing 1 nm thin $SrTiO_3$ layers. Note the almost Ising-like profile in the bottom panel.

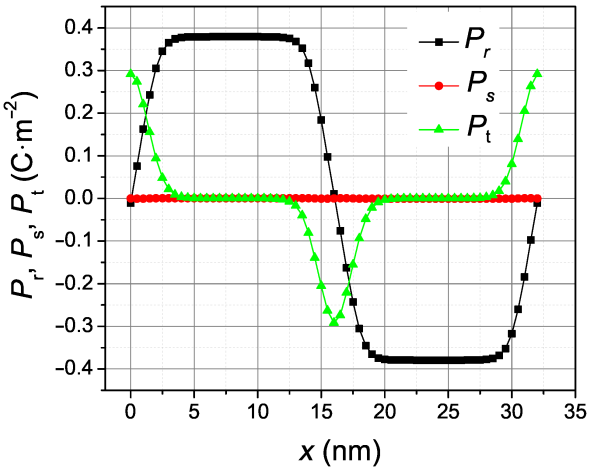

Figure 3: Relaxed profile of the polarization components across 180-degree ferroelectric wall in rhombohedral $BaTiO_3$.

The polarization profile relaxed within the $SrTiO_3$-containing superlattice layers as shown in Figure 5. When the domain wall is far away from the $SrTiO_3$ layer, the domain wall profile is barely modified, only the spontaneous polarization in the domain is somewhat reduced (by about 40%, see Figure 5a). In

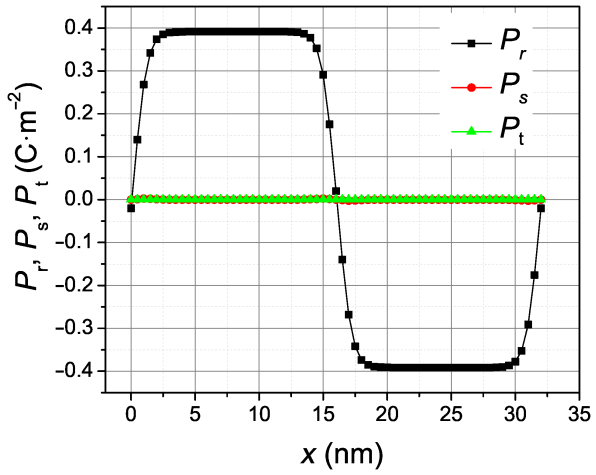

Figure 4: Relaxed profile of the polarization components across 180-degree ferroelectric wall in rhombohedral $BaTiO_3$ under epitaxial compressive stress of 3 GPa.

contrast, when the domain wall happens to be located right at the $SrTiO_3$ layer, the P_t component is suppressed considerably there (by more than 80% in Figure 5b). In other words, its Bloch character is strongly suppressed.

Similar calculations made in supercells of different sizes (Figure 6a) show a rather marginal dependence of the domain wall shape on the distance between domain walls. As a matter of fact, the suppression of P_t is a marked effect even when the next domain wall is only 4 nm away. The monotonous dependence shown in Figure 6a demonstrates that, for larger distances between domain walls, the amplitude ratio between the P_t component of the wall located at the $SrTiO_3$ layer and far away from it is even stronger. On the other hand, as expected, the suppression of the P_t component is very sensitive to the thickness of the $SrTiO_3$ layer. As is apparent from Figure 6b, as few as 2 nm of $SrTiO_3$ is in fact sufficient to suppress P_t completely.

In order to appreciate the height and shape of the well-formed potential by the 1 nm $SrTiO_3$ layer, we have also calculated the Landau energy contribution to the domain wall energy density as a function of the position of the domain wall, assuming that the shape of the profile of the domain wall is not modified while sliding across the $SrTiO_3$ layer. The result of this calculation, obtained numerically by integrating the Landau energy density, is shown in Figure 7. The calculation was made for the ideal profile of the Ising wall and Bloch wall of Figure 3 and Figure 4, subtracting the single-domain energy density in pure $BaTiO_3$ as a reference energy scale. Since the $SrTiO_3$ layer is thinner than the domain wall width, the width of the resulting potential energy well is mostly determined by the domain wall profile. A domain wall passing slowly through the $SrTiO_3$ layer would experience a potential well with a reduced energy depth, because the domain wall profile would adapt to the material inhomogeneity in order to reduce the energy costs. However, we expect that such a relaxed potential energy profile would be qualitatively similar to that of Figure 7. In fact, the total potential energy density increase achieved by displacing the Bloch wall away from the pinned position at the $SrTiO_3$ layer, obtained by the energy difference between the fully relaxed configurations shown in Figure 5, yields a quite considerable potential energy depth of about 6 mJ/m^2. In our simulations, the Bloch wall placed 1–7 nm away from the defect layer always spontaneously moved back to it.

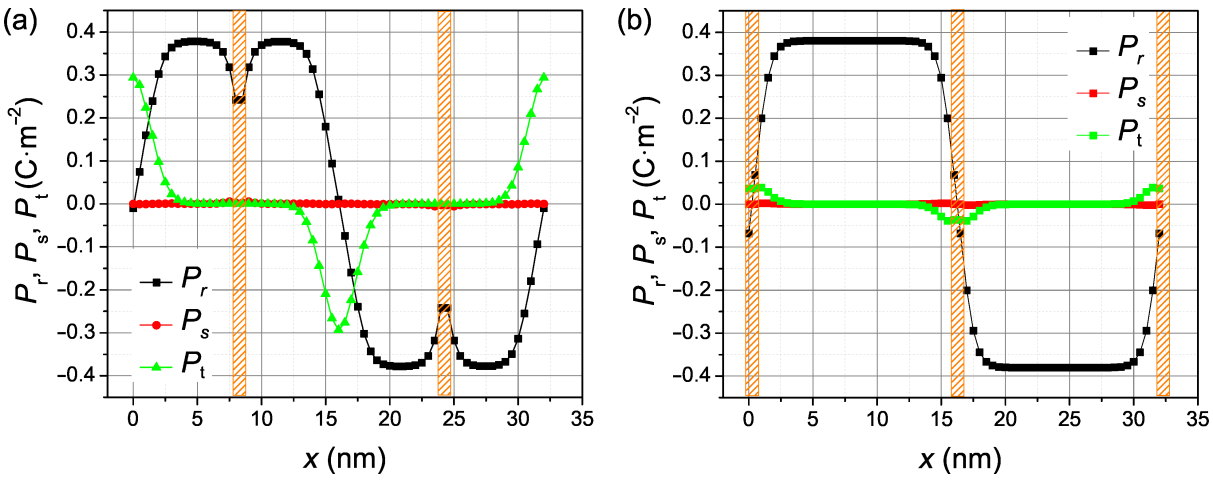

Figure 5: Relaxed profile of the polarization components across 180-degree ferroelectric walls in rhombohedral $BaTiO_3$ intercalated with 1 nm thin layers of $SrTiO_3$. (a) $SrTiO_3$ layer within the ferroelectric domain. (b) $SrTiO_3$ layer located at the ferroelectric domain wall.

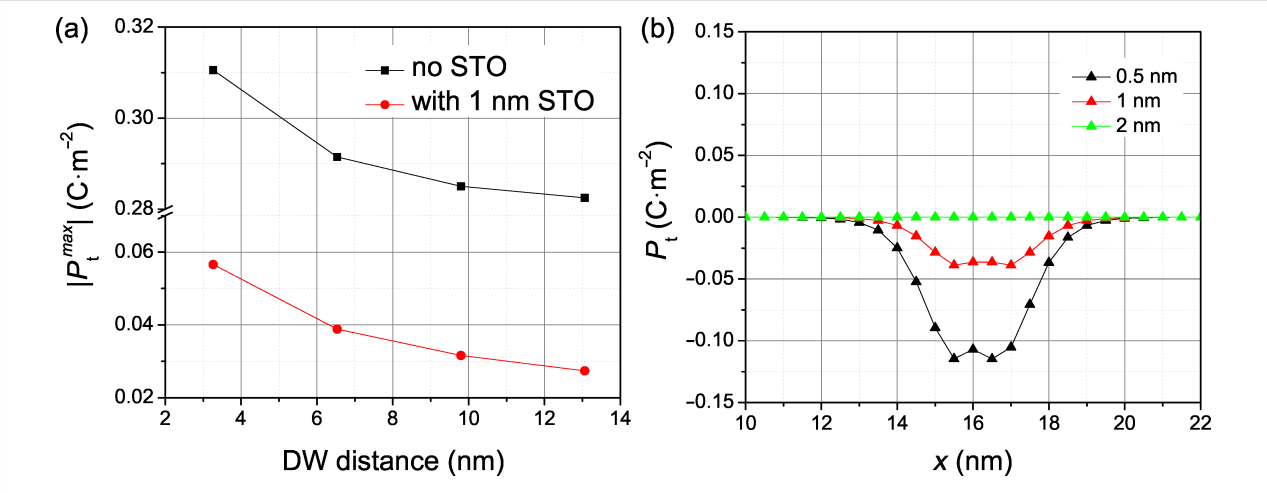

Figure 6: Variation of the P_t component (a) with increasing distance between domain walls and (b) with the thickness of the $SrTiO_3$ layer.

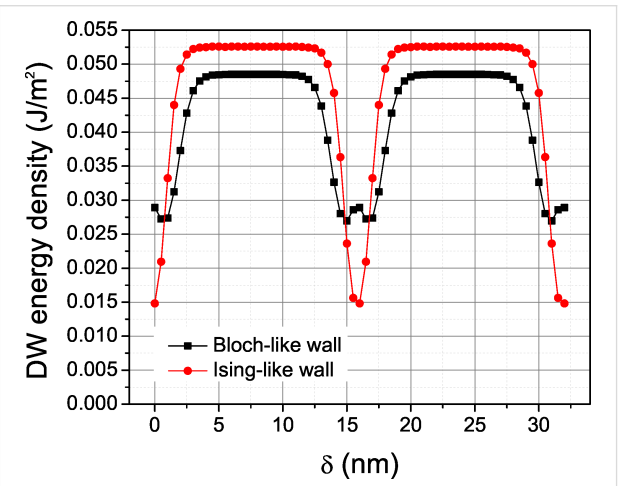

Figure 7: Landau part of the domain wall energy density as a function of the position of the ferroelectric domain wall, estimated by sliding a rigid polarization profile across the potential relief of the superlattice described in the text.

These simulations suggest that an approximately 1 nm thin $SrTiO_3$ layer incorporated in ferroelectric $BaTiO_3$ crystal is capable of considerably influencing the structure and properties of the 180-degree Bloch domain walls parallel to it. Since the domain wall has lower energy when located right at the $SrTiO_3$ layer, one can speculate that a pair of such layers can be used as a nucleation center for favoring antiparallel ferroelectric domain with desirable crystallographic orientation of adjacent domain walls. For example, one can choose the $[\bar{2}11]$ crystallographic direction, favorable for Bloch wall formation. It can also be used to pin domain walls already present in the material. Most interestingly, we have seen that the inner polarization of the Bloch wall would be substantially reduced while passing through the thin paraelectric layer. Thus, the layer acts as a bottleneck for the helicity order parameter of the wall.

Conclusion

In summary, since the Bloch character is strongly suppressed when the domain wall is right at the $SrTiO_3$ layer, the layer can facilitate selection of the sign of the P_t component, and therefore, selection of the sign of its helicity. As a matter of fact, in our simulations made without a $SrTiO_3$ layer, the application of an E_t electric bias to the Bloch domain wall either preserved its helicity or destroyed the wall completely. On the other hand, the Bloch domain wall located at the 1 nm thin $SrTiO_3$ layer could be easily switched with a 0.5 kV/mm electric field, as is apparent from the quasistatic hysteresis loop shown in Figure 8 (see below). In fact, the thickness of the $SrTiO_3$ layer can be tuned in a way that the wall passing through there is effectively in the state just below the phase transition from the Bloch to the Ising state. Then, as the domain wall passes through such a paraelectric layer, it should easily acquire the P_t component favored by even quite a moderate E_t electric bias. Thus, ferroelectric Bloch domain walls are shown to be ideal nanoscale objects with switchable properties. These findings are expected to inspire the design of functional properties of ferroelectric nanostructures.

Calculation Details

The domain wall structures displayed in Figures 3–5 fit in a 64 × 128 × 128 equidistant point mesh with 0.5 nm lattice spacing, forming a periodic simulation box with its the edges along the principal pseudocubic crystallograpic axes (see Figure 8).

The $BaTiO_3$ and $SrTiO_3$ Ginzburg–Landau–Devonshire model potential parameters used in the present calculations are those of [12], except for the temperature parameter, which was set to 118 K here (low temperature is needed to drive $BaTiO_3$ into the rhombohedral ferroelectric phase). Phase-field simulations for

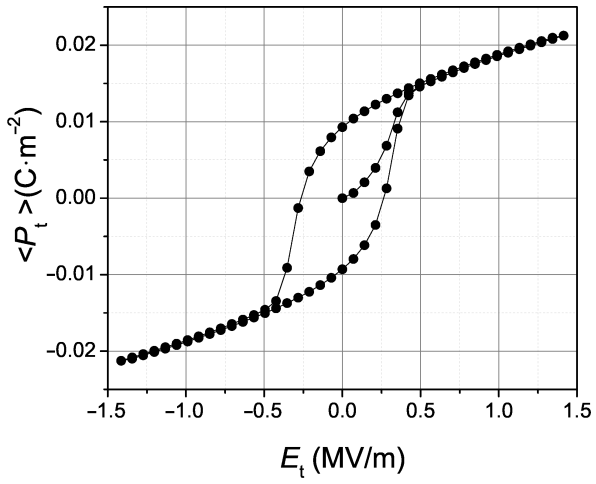

Figure 8: Calculated hysteresis loop demonstrating switching of the P_t component of the Bloch wall located at a 1 nm thin $SrTiO_3$ layer. The indicated value of the polarization P_t is averaged over the whole supercell shown in Figure 1b.

pure $BaTiO_3$ single crystal and for the $BaTiO_3$–$SrTiO_3$ crystalline superlattice at stress-free mechanical conditions were performed using the phase-field simulation code ferrodo [8]. The approximate profile of the ferroelectric Bloch wall is known from the previous calculation and this knowledge could be conveniently used for setting the initial conditions for the present phase field simulations. In particular, the initial conditions were set in a way to favor the orientation, distance and the location of the walls in the simulation box, but there were no real constrains introduced there, only the natural limitations resulting from the standard protocol of simulated annealing procedure, governed by the time-dependent Ginzburg–Landau equation. The hysteresis loop shown in Figure 8 has been calculated quasistatically, from a sequence of configurations relaxed under fixed bias electric fields, similarly as in [12]. The initial state had two domain walls with opposite P_t values, as in Figure 3, then the electric field was gradually increased, decreased and increased again to form a whole polarization cycle. In the saturated states, P_t values in the two domain states had the same magnitude and sign.

Acknowledgements

This work was supported by the Czech Science Foundation (project no. 15-04121S) and by Operational Programme Research, Development and Education financed by European Structural and Investment Funds and the Czech Ministry of Education, Youth and Sports (Project No. SOLID21 - CZ.02.1.01/0.0/0.0/16_019/0000760). The authors warmly acknowledge long-term maintenance and user support of ferrodo code by Pavel Marton.

ORCID® iDs

Vilgelmina Stepkova - https://orcid.org/0000-0002-5497-7592
Jiří Hlinka - https://orcid.org/0000-0002-9293-4462

References

1. Stephanovich, V. A.; Luk'yanchuk, I. A.; Karkut, M. G. *Phys. Rev. Lett.* **2005,** *94,* 047601. doi:10.1103/physrevlett.94.047601
2. Wu, P.; Ma, X.; Li, Y.; Eom, C.-B.; Schlom, D. G.; Gopalan, V.; Chen, L.-Q. *Appl. Phys. Lett.* **2015,** *107,* 122906. doi:10.1063/1.4931129
3. Li, Y. L.; Hu, S. Y.; Tenne, D.; Soukiassian, A.; Schlom, D. G.; Xi, X. X.; Choi, K. J.; Eom, C. B.; Saxena, A.; Lookman, T.; Jia, Q. X.; Chen, L. Q. *Appl. Phys. Lett.* **2007,** *91,* 112914. doi:10.1063/1.2785121
4. Nakhmanson, S. M.; Rabe, K. M.; Vanderbilt, D. *Phys. Rev. B* **2006,** *73,* 060101. doi:10.1103/physrevb.73.060101
5. Neaton, J. B.; Rabe, K. M. *Appl. Phys. Lett.* **2003,** *82,* 1586–1588. doi:10.1063/1.1559651
6. Marton, P.; Rychetsky, I.; Hlinka, J. *Phys. Rev. B* **2010,** *81,* 144125. doi:10.1103/physrevb.81.144125
7. Taherinejad, M.; Vanderbilt, D.; Marton, P.; Stepkova, V.; Hlinka, J. *Phys. Rev. B* **2012,** *86,* 155138. doi:10.1103/physrevb.86.155138
8. Marton, P.; Hlinka, J. *Phase Transitions* **2006,** *79,* 467–483. doi:10.1080/01411590600892351
9. Ondrejkovic, P.; Marton, P.; Guennou, M.; Setter, N.; Hlinka, J. *Phys. Rev. B* **2013,** *88,* 024114. doi:10.1103/physrevb.88.024114
10. Hu, H.-L.; Chen, L.-Q. *J. Am. Ceram. Soc.* **1998,** *81,* 492–500. doi:10.1111/j.1151-2916.1998.tb02367.x
11. Stepkova, V.; Marton, P.; Hlinka, J. *J. Phys.: Condens. Matter* **2012,** *24,* 212201. doi:10.1088/0953-8984/24/21/212201
12. Stepkova, V.; Marton, P.; Setter, N.; Hlinka, J. *Phys. Rev. B* **2014,** *89,* 060101. doi:10.1103/physrevb.89.060101

License and Terms